E. Somma
B. Loppinet
G. Fytas
S. Setayesh
J. Jacob
A. C. Grimsdale
K. Müllen

Collective orientation dynamics in semi-rigid polymers

E. Somma · B. Loppinet · G. Fytas (✉)
FO.R.T.H/Institute of Electronic Structure
and Laser, P.O. Box 1527,
71110 Heraklion, Greece
E-mail: fytas@iesl.forth.gr

S. Setayesh · J. Jacob
A. C. Grimsdale · K. Müllen · G. Fytas
Max Planck Institute for Polymer
Research, P.O. Box 3148, 55021 Mainz,
Germany

Abstract The orientational relaxation function in non-dilute isotropic solutions of semi-rigid polymers with different ladder-type oligo-phenylene monomer structures is recorded by time domain depolarized light scattering. The shape and the peculiar dependence of this function on the scattering angle arise from the coupling between orientational and shear translational motions. At sufficiently high concentrations, this coupling facilitates the opening of a faster relaxation channel better resolved in the forward scattering. The overall shape of the relaxation function is concentration-dependent, and the strength of the coupling appears to be system-specific.

Introduction

Substituted polyfluorenes have emerged as important organic optoelectronic materials [1] and their performance in emerging applications relates to their monomer chemical structure, shape persistence, and molecular interactions. The isotropic properties of a gem-dialkyl-substituted polyfluorene [poly(9,9-bis(2-ethylhexyl)fluorene, PF2/6] in solution studied by polarized scattering conform to the behavior of semi-flexible polymers with a persistence length (l) of 7 nm [2]. The collective orientation dynamics, however, sensitively probed by depolarized light scattering are much more complex. The relaxation function $C(q,t)$ of the orientational order parameter fluctuations with wave vector q was found to be bimodal displaying a peculiar q-dependence.

Recently, these heterogeneous orientation dynamics were attributed [3] to non-random spatial orientation correlations due to anisotropic interactions leading to an effective rotation–translation coupling [4]. The latter introduces a fast relaxation channel into $C(q,t)$, in addition to the pure collective rotational motion, probed in the forward scattering. Hence, it is the scattering angle θ and not q that matters (for short-range correlations), and $C(q,t)$ decays faster at low θ values. The disparity between the decay rates of $C(q,t)$ in the forward and back scattering relates to the strength of the rotation–translation coupling. This is not an exclusive property of polymers. It is well known that anisometric small molecules exhibit a characteristic central dip in the depolarized spectrum $I_{VH}(q,\omega)$ (the Fourier transform of $C(q,t)$) in the MHz–GHz frequency range [5]. Inherent properties of the polymeric nature are, however, the

non-exponential shape of both processes in $C(q,t)$, the slow dynamics, and the high strength of the coupling parameter R (≈ 0.8).

Here we extend the first study to two new shape-persistent polymers, poly(tetra(2-ethylhexyl)indenofluorene) (TEHIF) and the poly(ladder-type pentaphenylene) (PLPP), with different monomer structures related to fluorene (Table 1). These polymers were chosen as they were expected to show greater rigidity than PF2/6 with optical anisotropy on the backbone, and in the case of PLPP, partly also on the side group. By comparing these with PF2/6 we aimed to address the unresolved effects of concentration, chain length, and the monomer structure upon the characteristic properties of $C(q,t)$. The speeding up of the pure orientational dynamics as a result of the coupling to shear modes of molecular motion appears well above the overlap concentration. The overall shape of $C(q,t)$ is not affected by the coupling and is concentration-dependent. The unimodal shape of the pure orientational relaxation function resolved in the back scattering is preserved in the forward scattering function only at concentrations close to the phase separation.

Experimental

The syntheses of poly(9,9-bis(2-ethylhexyl)fluorene) (PF2/6) [6], poly(tetra(2-ethylhexyl)indenofluorene) (TEHIF) [7], and poly(ladder-type pentaphenylene) (PLPP) [8] are described elsewhere. The polymer structure and characteristics [weight-average molar mass (M_w), polydispersity (M_w/M_n), contour length (L_w), persistent length (l), and overlap concentration (c^*)] are shown in Table 1.

The orientation relaxation function $C(q,t) = [(G(q,t)-1)/f^*]^{1/2}$ of the isotropic polymer/toluene solutions were computed from the experimental time correlation function $G(q,t) = <I(q,t)I(q,0)>/|<I(q)>|^2$ of the depolarized (VH) light scattering intensity $I(q,t)$ at a wave vector $q = (4\pi n/l)\sin(\theta/2)$. f^* is an instrumental factor, the laser wave length (λ) is 532 nm, n is the refractive index of the solution, θ is the scattering angle, and time (t) ranges from 10^{-7} to 10^3 s. In the presence of non-exponential decay, the analysis of the high-quality $C(q,t)$ usually proceeds either via inverse Laplace transformation leading to the distribution relaxation function or by using the stretched exponential representation,

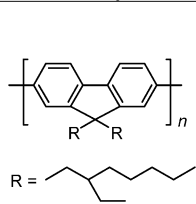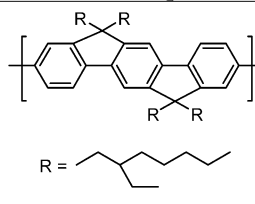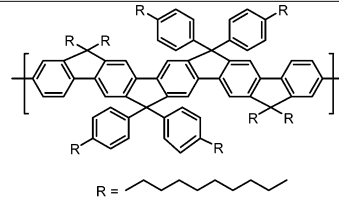$$C(q,t) = \alpha_1 \exp{(-t/\tau_i)}^{\beta_i} \qquad (1)$$

where α_i is the amplitude, τ_i a characteristic relaxation time, and the shape parameter (β_i) is a measure of the width of the distribution of relaxation times. The intensity of the contributing mechanism is computed from $I_i(q) = \alpha_i(q)I(q)$ where $I(q)$ is the time-averaged total light scattering intensity normalized to a standard (toluene).

Results and discussion

Coupling to the shear flow

Figure 1 shows the experimental $C(q,t)$ of PF2/6 (89 kDa) in toluene at 33.34 wt% for seven scattering

Table 1 Polymer structures and sample characteristics[a]

Polymer structures and sample characteristics [a]

	PF2/6		TEHIF	PLPP
M_w (g/mol)	253k	89k	64k	241k
M_w/M_n	1.22	1.63	1.38	1.82
L_w (nm)	490	171	106	293
l (nm)	7	7	8	25
c^*(g/cm³)[b]	$9.5*10^{-4}$	$1.7*10^{-3}$	$1.7*10^{-3}$	$2.6*10^{-4}$

a) From Light scattering and GPC
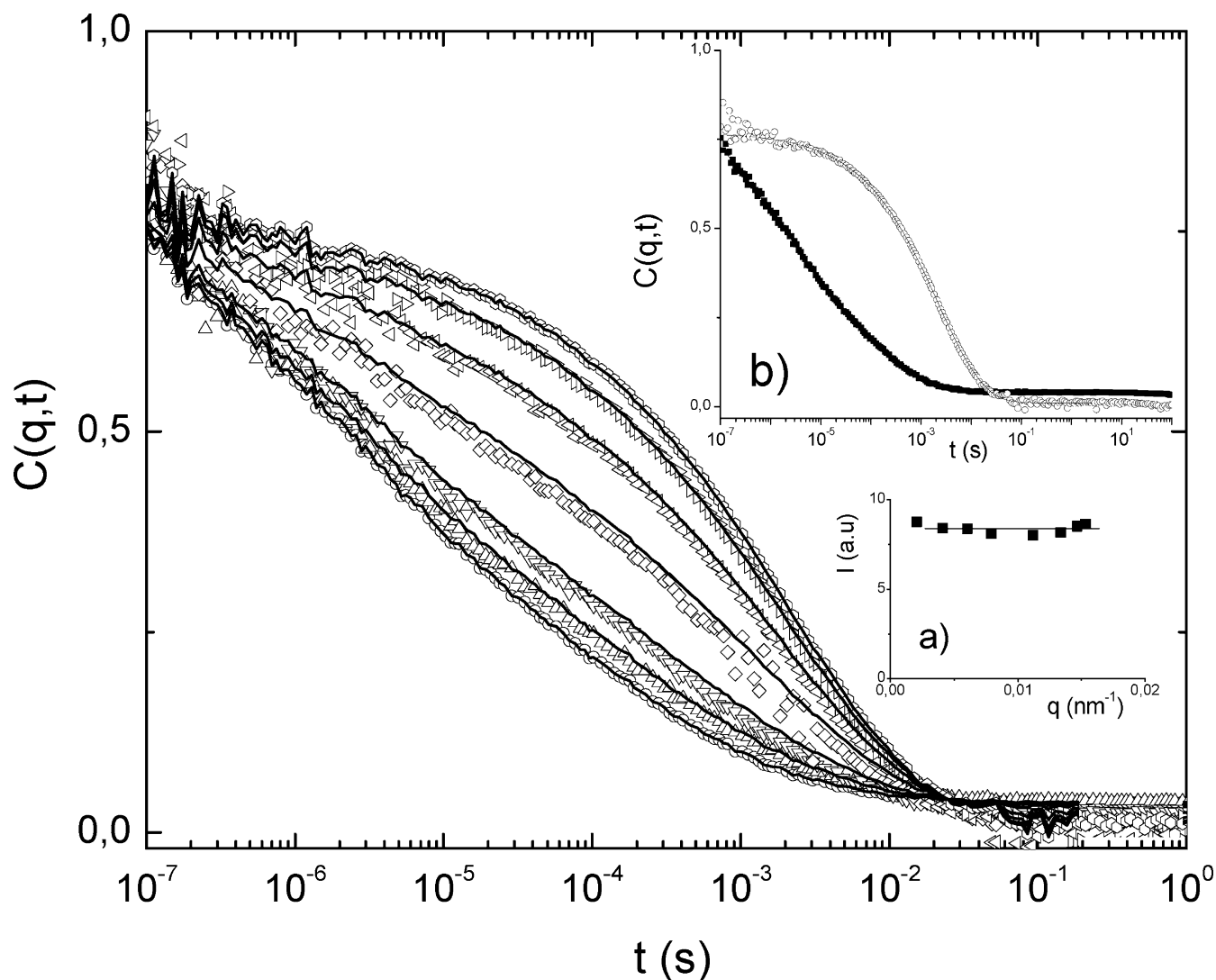b) Based on $L_e = \{2l^2[L/l-1+\exp(-L_w/l)]\}^{1/2}$

Fig. 1 Experimental orientation relaxation functions $C(q,t)$ at different scattering angles (θ) from 15° to 150° (from *left* to *right*) for a 33.34 wt% solution of PF2/6 (89 kDa) in toluene at 20°C. The *solid lines* denote the representation of the experimental functions by Eq. (2) without adjustable parameters using $C(q,t)$ at the extreme angles as reference. *Inset a* The total time-averaged depolarized light scattering intensity as a function of the scattering vector q. *Inset b* The extrapolated forward (■) and back (O) scattering functions represented (*solid lines*) by Eq. (1)

angles from 30° to 150° at 20°C. The pertinent observation is the counterintuitive slowing down of $C(q,t)$ with increasing q, in contrast to the common diffusion-like motions. As previously noted [3] this apparently intriguing evolution can easily be understood by employing the equation

$$C(q,t) = f_{\text{f}}(t)\cos^2(\theta/2) + f_{\text{b}}(t)\sin^2(\theta/2) \qquad (2)$$

where $f_{\text{f}}(t)$ and $f_{\text{b}}(t)$ are the forward ($\theta = 0°$) and backward ($\theta = 180°$) components of $C(q,t)$, respectively. By using two reference angles (30° and 150°), $f_{\text{f}}(t)$ and $f_{\text{b}}(t)$ can be extrapolated and then all the orientation relaxation functions at intermediate angles can be reproduced. Indeed, the experimental $C(q,t)$ of Fig. 1 extended over six decades in time are well described by Eq. (2), as shown by the solid lines. These are computed from Eq. (2) without any assumption and any adjustable parameter of the shape of the forward and back scattering functions (upper inset to Fig. 1). The total depolarized scattering intensity I_{VH} (inset to Fig. 1) for PF2/6 is independent of q, which is indicative of short-range orientational order, that is, $q\xi \ll 1$, where ξ is the correlation length of the orientation fluctuations. This low scattering vector limit validates the use of the simple q-independent relationship (2), that is, $f_{\text{f}}(q,t) \equiv f_{\text{f}}(t) f_{\text{b}}(q,t) \equiv f_{\text{b}}(t)$.

In isotropic solutions with random molecular orientation, the back and forward scattering function $C(q,t)$ in the limit $q\xi \ll 1$ should be identical. The observed differentiation can be explained by the coupling of the
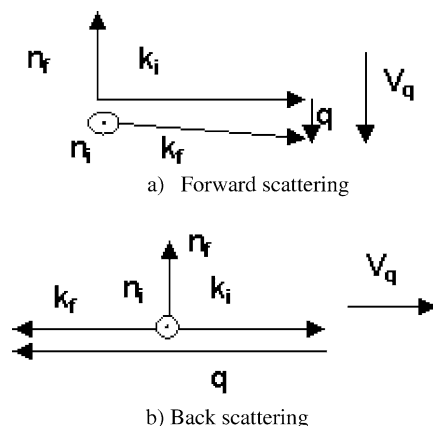
a) Forward scattering

b) Back scattering

Fig. 2a,b Schematic explanation of the origin of the different information in the back (**a**) and forward (**b**) scattering geometries expressed in Eq. (2). To affect the depolarised light scattering the flow velocity must lie along q and in the plan (n_i,n_f). This is achieved in **b**, whereas the flow component probed in **a** is not "depolarized active". k_i and k_f are the incident and scattered wave vectors, respectively; n_i and n_f are the directions of the incident and scattered electric field, respectively; $q=k_i-k_f$ is the scattering wave vector; and V_q is the component along q of the flow velocity

rotational motion with the shear modes leading to the speed up of the former along the shear flow as schematically rationalized in Fig. 2. This modification is "depolarized active" in the forward scattering, since the shear-induced effect is optimally probed, that is, $qv \neq 0$, with v being the shear flow velocity and the scattered field polarization is parallel to q. The advantage of dynamic anisotropic light scattering is that it enables the measurement of this physical phenomenon at equilibrium without macroscopic flow.

This coupling has been addressed for small anisotropic molecules [5] using the orientational order parameter $Q_{\alpha\beta}$ (a symmetric traceless second-rank tensor). The explicit dependence of $C(q,t)$ can occur only in the presence of the coupling of Q_{xy} with shear modes along q where $qv \neq 0$. By taking the z-axis along q, $f_b(t) \equiv <Q_{xy}(q,t)Q^*_{xy}(q,0)>$ probes the pure collective orientation relaxation function, and $f_f(t) \equiv <Q_{yz}(q,t)Q_{yz}^*(q,0)>$ probes the coupled mode. The weighting of the different forward and back scattering functions with the simple geometrical factors in Eq. (2) suffices for the description of $C(q,t)$ at any intermediate scattering angle. We next address the shape of the two constituent relaxation functions in the investigated solutions.

Pure rotational dynamics

The extrapolated back scattering $f_b(t)$ relaxations for five PF2/6 (253 kDa)/toluene solutions are shown in Fig. 3a. While at the highest concentration $f_b(t)$ is well repre-

sented by Eq. (1) (solid lines), this is not the case for the $f_b(t)$ at lower concentrations. At shorter times, there is an additional fast contribution to $f_b(t)$ which remarkably is better resolved at the lowest concentration. This was not the case in poly(n-hexylisocyanate) (PHIC)/toluene isotropic solutions [3] which display transition-induced depolarized scattering. To adequately describe the main component of $f_b(t)$, this relaxation function is represented by a double stretched exponential function [Eq. (1)] consistently at all concentrations (solid lines in Fig. 3a). In the fitting procedure, the known intercept of $\alpha_b = f_b(0)$ was used as a fixed parameter.

The non-exponential shape of the slow component of $f_b(t)$, as reflected in the value of $\beta_b = 0.54$–0.05 over the examined concentration range, is an inherent polymeric property due to the various rotational relaxation times and the length polydispersity. In fact, the relaxation time τ_b which slows down with concentration (Fig. 4b) is assigned to the chain overall orientation following the concentration dependence of the shear viscosity [2]. In the same context, the shape of the slow component of $f_b(t)$ in PF2/6 (89 kDa) with polydispersity $M_w/M_n = 1.63$ is broader ($\beta_b = 0.45$ in Fig. 1b) than for PF2/6 (253 kDa, $M_w/M_n = 1.22$). The reduced intensity of this slow process $I_b = \alpha'_b I/c$, where α'_b is the amplitude of the slow component of $f_b(t)$ and I the q-independent total depolarized light scattering intensity, increases with the polymer concentration as shown in Fig. 4a (■). This reflects an enhancement of the (positive) orientational correlations with increasing concentration. However, this increase of I_b is still far from being critical [2, 3].

Coupling effect

The new feature of the orientation relaxation function $C(q,t)$ in the non-dilute solutions of semi-rigid polymers is the ability for faster collective rotational motion via the effective coupling to the shear modes best resolved in the forward scattering. Fig. 3b shows the extrapolated $f_f(t)$ at $\theta = 0°$ for the PF2/6 (253 kDa) solutions of Fig. 3a based on Eq. (2) using the experimental $C(q,t)$ at $\theta = 30°$ and 150°. $f_f(t)$ displays two distinct features compared to $f_b(t)$: (i) it is faster, as in PF2/6 (89 kDa) and PHIC, and (ii) it displays different shape, unlike in PHIC. Here the bimodal nature of $f_f(t)$ is more pronounced than in $f_b(t)$ (Fig. 3a) at the same concentration. The qualitatively different forward and back scattering functions are demonstrated at the lowest concentration in Fig. 3 where the slow process in $f_f(t)$ is hardly visible, as if the main rotational process in $f_b(t)$ were inactive at $\theta = 0°$ while the total I/c is q-independent. In the absence of rotational–translational coupling, the two functions look alike. Prior to a rationalization of the intriguing feature (ii), we need to quantify the coupling effect.

Fig. 3a,b Orientation relaxation functions $C(q,t)$ at 20°C for back ($\theta = 180°$) (**a**) and forward ($\theta = 0°$) (**b**) depolarized light scattering from PF2/6 (253 kDa)/toluene solutions at four (6.5, 15, 25.4, 30, and 40.4 wt%) concentrations increasing (from *left* to the *right*). The *solid lines* denote a double stretched exponential [Eq. (1)] fit to the experimental $C(q,t)$
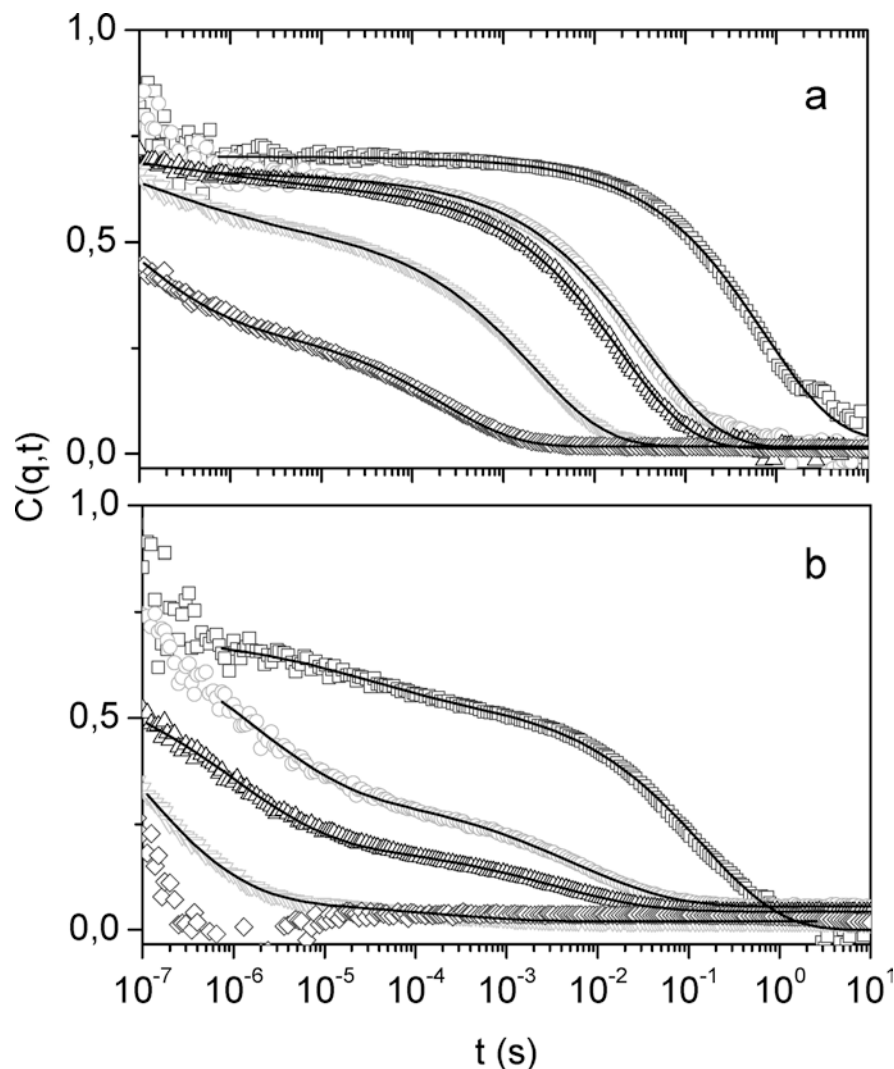
The representation (solid lines) proceeds via the double stretched exponential [Eq. (1)] with a fixed total amplitude ($\alpha_f = \alpha_b$) dictated by the q-independent total intensity (e.g., Fig. 1a). The slow process in $f_f(t)$ is somewhat broader ($\beta_f = 0.45$) than the corresponding process in $f_b(t)$ and exhibits a concentration-dependent amplitude $\alpha'_f < \alpha'_b$; the fast process of $f_f(t)$ bears the amplitude $\alpha_f - \alpha'_f$. The intensity $I_f = \alpha'_f I/c$ associated with the coupling process depends strongly on concentration, as shown in Fig. 3a in comparison with I_b (solid squares). Therefore the unexpected disparity in the overall shape of the two relaxation functions [i.e., feature (ii)] results from the reduced partition of the slow rotation in the presence of the coupling ($I_f < I_b$). The relaxation time τ_f shown in Fig. 4b is about three times faster than the pure chain rotational time τ_b [in ref. [3] (Fig. 3b), the reported ratio τ_b/τ_f was too high due to the incorrect assignment of the fast mode) over the examined c-range. The insensitivity of τ_b/τ_f to the concentration variation indicates that the same viscosity determines both times.

In the case of liquids of small anisometric molecules, where the coupling between rotational and translational motions has been treated theoretically in the limit $q\xi \ll 1$, the strength of the coupling $R = 1 - (\tau_f/\tau_b)$ was found to vary from 0.25 to 0.45 [5]. Based on this expression the times in PHIC and PF2/6 yield clearly higher R values (≈ 0.7) [3]. While the strength R is found to be insensitive to the variation of concentration (Fig. 4), activity of the slow relaxation channel of $f_f(t)$ in the overall relaxation of $Q_{\alpha\beta}$, as expressed by the intensity ratio $I_f/I_b = \alpha'_f(c)/\alpha'_b(c)$, strongly increases with concentration. The validity of Eq. 2, however, implies that the partition of the fast relaxation channel $f_f(t)$ increases with decreasing concentration (Fig. 3). Even though no lyotropic phase separation is clearly observed, the PF2/6/toluene solution undergoes a phase separation above about 40 wt% and becomes opaque. It is conceivable that the
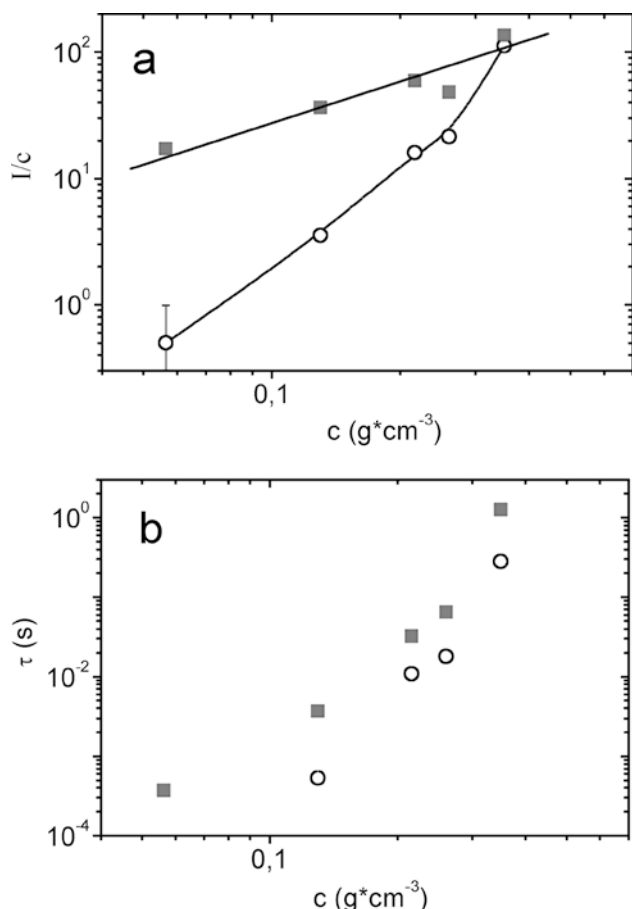
Fig. 4 a,b The concentration dependence of the reduced depolarized light scattering intensity I_f/c and I_b/c (**a**) and the relaxation times τ_b and τ_f (**b**) of the two processes in the back (■) and forward (O) scattering functions of Fig. 3

enhancement of the anisotropic interactions of shape-persistent polymers with increasing concentration ($I_b(c)$ in Fig. 4) facilitates the rotational relaxation via the slow process of $f_f(t)$. In fact, this behavior is displayed by the PHIC solutions near the lyotropic transition [3].

To account for the very fast decay in the experimental $C(q,t)$ with a pronounced contribution in the forward scattering (Figs. 1b and 3b), the functions $f_f(t)$ and $f_b(t)$ at the extreme angles are taken to be bimodal. This appears also to be the case for semi-rigid poly(*para*-phenylene)s in contrast to the unimodal functions in PHIC solution (Figs. 2 and 3a in ref. [3]). Since the optical anisotropy of PF2/6 originates from the chain backbone [2], segmental and/or chain flexure dynamics might relate to the fast decay of $C(q,t)$. Furthermore, the non-exponential shape of this fast decay in Fig. 3b at $c \geq 15$ wt% might arise from inter-chain interactions in addition to intra-chain correlations. The presence of optically anisotropic side groups (e.g., in PLPP) is expected to enhance these fast orientation dynamics [9].

The ability to speed up the rotational motion via its coupling to shear modes of collective molecular motion probed along q is also displayed by the new fluorene polymers in Table 1 as depicted in Fig. 5. The relaxation function $C(q,t)$ for both systems at intermediate angle $\theta = 90°$ is well described by Eq. (2) where the two functions $f_f(t)$ and $f_b(t)$ are the extrapolated forward and back scattering functions without any adjustable parameters. This comparison is visualized only for the PLPP/toluene solution at 10.1 wt% in Fig. 5 (main panel). The two functions display a very broad shape, since they extend over a very broad time range: both $f_b(t)$ and $f_f(t)$, are represented by Eq. (1) using $\alpha_f = \alpha_b = 0.9$ and very similar shape parameters $\beta_b = \beta_f = 0.25$. This very broad distribution of orientation times in PLPP as compared to PF2/6 is partly due to the high polydispersity ($M_w/M_n = 1.83$) and the contribution of the optically anisotropic side group motions in the former system. Following the same procedure, the corresponding functions (inset to Fig. 4) in TEHIF ($M_w/M_n = 1.48$) are described by $\beta_b = \beta_f = 0.41–0.03$ and hence are clearly narrower than in PLPP. It is worth mentioning that both PLPP and TEHIF/toluene solutions in Fig. 5 are close to the phase separation boundary (10 wt% and 8 wt% respectively at 20°C) and the unimodality of the constituent functions of Eq. (2) is preserved.

The speeding up of the rotational motion through the coupling in the three systems (Table 1 and Figs. 3 and 4) is reflected in the ratio $\tau_b/\tau_f = 3–1$ in PF2/6, 5–1 in TEHIF, and 25–4 in PLPP. In the Landau-de Gennes macroscopic description of the order parameter fluctuations [4], R is calculated from the shear viscosity η and the two viscosities v and μ determining the pure rotational τ_b and the flow birefringence, respectively, by the relationship $R = 2\mu^2/(\dot{v}\eta)$. For PF2/6, τ_b follows the concentration dependence of the shear viscosity [2], and hence the ratio v/η should be constant. Since R ($= 1 - \tau_f/\tau_b$) was also found to be virtually constant over the examined concentration range, then the variation of $\mu(c)$ should accordingly resemble $\eta(c)$. Finally, the systematic variation of R from the simple PF2/6 to the complex PLPP structure might be attributed to disparities in μ. Experimental verification of the latter will require further flow birefringence experiments.

Conclusions

The anisotropic scattering functions $C(q,t)$ in three new semi-rigid phenylene-based polymers have provided strong evidence of an additional relaxation channel that can facilitate the orientational order parameter fluctuations in sufficiently non-dilute solutions. Experimentally, $C(q,t)$ in the forward scattering relaxes counterintuitively faster than in the backscattering where the pure collective rotational dynamics are probed. It is in the

Fig. 5 Orientation relaxation functions of PLPP (10.1 wt%) (*main panel*) and TEHIF (5.1 wt%) (*inset*) solutions in toluene at 20°C. The *solid line* denotes the representation of the experimental function at $\theta = 90°$ (Δ) by Eq. (2) using the forward ($\bigcirc$) and back ($\square$) anisotropic scattering functions without adjustable parameters. *Inset* forward ($\bullet$) and the back ($\blacksquare$) scattering functions in TEHIF
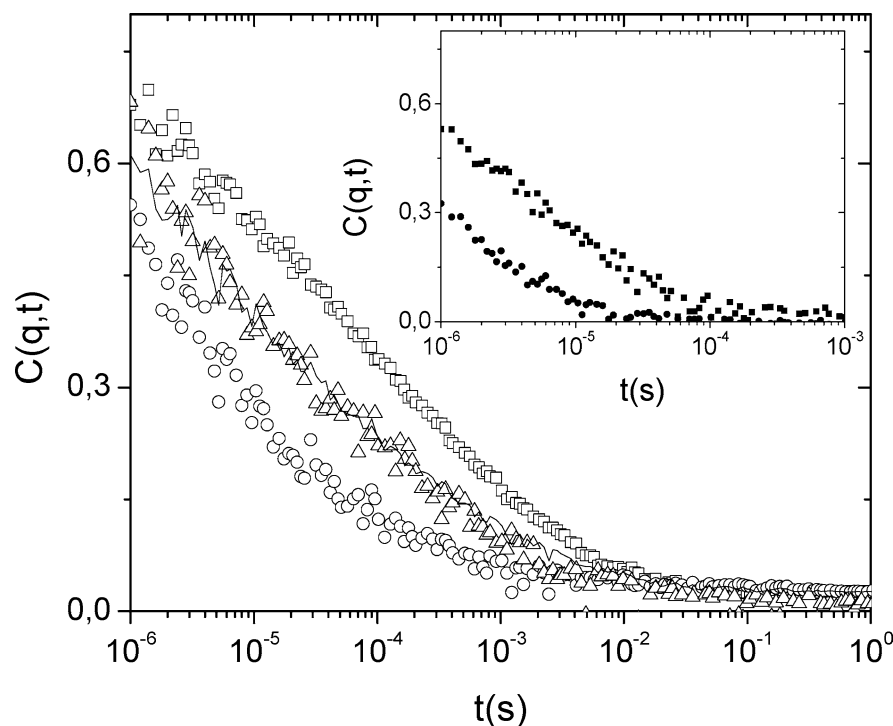
former geometry that the coupling between orientational and spontaneous shear flow along the *q*-direction is optimally resolved. Then, the validity of Eq. (2) is a straightforward consequence of the depolarized light scattering geometry, and in the absence of coupling forward and back scattering functions are identical.

The phenomenological description of the new effect is summarized in the following solid findings: a) the speeding up of the pure rotational relaxation function $f_b(t)$ in five persistent polymers investigated so far defines the system-dependent coupling parameter; b) the coupling-induced transformation of $f_b(t)$ can be also associated with a change of the overall shape of the effective relaxation function $f_f(t)$ if more than one process contributes to $f_b(t)$. In this case the molecular mechanisms are weighted differently in the presence of rotational–translational coupling. Only if one process prevails (at concentrations close to the phase boundary) in an unimodal $f_b(t)$ do the two functions look alike with $f_f(t)$ being faster.

The investigation of the complex orientation dynamics of stiff chains compared to liquids of small anisometric molecules will elucidate the role of the anisotropic interactions and provide the necessary phenomenology to develop a molecular theory.

References

1. Neher D (2002) Macromol Rapid Commun 22:1365; Scherf U, List EJW (2001) Adv Mat 14:477
2. Fytas G, Nothofer H, Scherf U, Vlassopoulos D, Meier G (2002) Macromolecules 35:481
3. Loppinet B, Fytas G, Petekidis G, Sato T, Wegner G (2002) Eur Phys J E8:461
4. de Gennes PG (1974) The physics of liquid crystals. Oxford University Press; de Gennes PG (1971) Mol Cryst Liq Cryst 12:193
5. Berne BJ, Pecora R (1976) Dynamic light scattering. Wiley, New York, chap 10; Alms GR, Gierke TD, Patterson GD (1978) J Chem Phys 67:5779; O'Steen BL, Wang CH, Fytas G (1984) J Chem Phys 80:3774; Ueno T, Sakai K, Tagaki K (1996) Phys Rev E54:6457; Dreyfus C, Aouadi A, Pick RM, Berger T, Patkowski A, Steffen W (1999) Eur Phys J B9:401
6. Grell M, Knoll W, Lupo D, Maeisel A, Miteva T, Neher D, Nothofer H-G, Scherf U, Yasuda A (1999) Adv Mater 11:671
7. Setayesh S, Marsitzky D, Müllen K (2000) Macromolecules 33:2016
8. Jacob J, Sax S, Piok T, List EJW, Grimsdale AC, Müllen K (2004) J Am Chem Soc (accepted)
9. Bockstaller M, Fytas G, Wegner G (2001) Macromolecules 34:3497